

Interaction-induced anisotropy in the onion-to-vortex transition in dense ferromagnetic nano-ring arrays

E. Tadmor,¹ Y. J. Rosen,² Ivan K. Schuller,² and S. Bar-Ad¹

¹Raymond and Beverly Sackler School of Physics and Astronomy, Tel-Aviv University, Tel-Aviv 69978, Israel

²Physics Department, University of California, San Diego, La Jolla, California 92093, USA

(Received 28 September 2012; accepted 9 October 2012; published online 19 November 2012)

We show that the onion-to-vortex switching field in dense arrays of nanostructured ferromagnetic rings is strongly dependent on the angle between the applied magnetic field and the array's main axis. The variations in switching field of up to 8 mT are connected to the anisotropy produced by dipolar interactions between domain walls in the rings. The interactions stabilize the onion state in aligned arrays but assist domain wall rotation and onion-to-vortex switching in rotated arrays. These results are established using magneto optical Kerr effect measurements of major and minor hysteresis loops together with micromagnetic simulations. © 2012 American Institute of Physics. [<http://dx.doi.org/10.1063/1.4765649>]

I. INTRODUCTION

Nano sized ferromagnetic elements are attracting considerable attention due to numerous potential applications such as high density memory devices and sensors. They are also of interest because domain wall physics plays a large role on that scale. Out of the various shapes under study, ferromagnetic rings are of special importance due to their transition from a dipole-like state (also known as “onion” state), to a stable vortex state close to remanence. The magnetic vortex configuration is useful for studies of dense arrays and creating reproducible switching fields, since it introduces almost no stray field and is insensitive to element edge roughness.¹ The majority of the research on ferromagnetic rings in the past decade has focused on the effect of the ring geometry on the magnetic properties. These studies produced phase diagrams for possible stable configurations,^{2,3} switching processes and fields,^{4,5} and domain wall shapes.⁶

However, the magnetic properties of the arrays may also be strongly affected by the interactions between the individual elements. Strong interactions between elements, such as those caused by the dipolar interaction, may result in irreproducible switching. These interactions are strongly dependent on the edge to edge distance between elements. Although this was studied in 1- and 2-dimensional arrays,^{7–10} very little, if any, attention was paid to the orientation of the ring array relative to the external magnetic field. While the hysteresis loop of a single ring is expected to be rotationally invariant, the array geometry may not be.¹¹

Here, we study the effect of the array orientation relative to the applied magnetic field on the onion-to-vortex switching process. We show experimentally that magnetic interactions between rings add a strong angle-dependent effect that can hinder or assist the switching process, and change the applied field needed for its initiation. This effect should be taken into account when considering different applications for dense ferromagnetic arrays.

II. METHODOLOGY

The experiments were conducted using four different square arrays of 20 nm thick Permalloy rings. Samples were fabricated on Si substrates using electron beam lithography and evaporation. The first array, array (i), consists of rings with an outer radius of 290 nm, an inner radius of 120 nm, and array periodicity of 660 nm. The other three arrays, (ii)-(iv), consist of rings with an outer radius of 310 nm, inner radius of 100 nm, and array periodicities of 660 nm, 930 nm, and 1860 nm. Electron microscopy of the arrays and their dimensions is presented in Fig. 1.

We measured major and minor magnetization hysteresis curves of the array using the magneto optical Kerr effect (MOKE), with a focused laser spot illuminating the entire array. The external magnetic field \vec{H} is applied using a dipole electromagnet in the plane of the sample and in the reflection plane, to measure the longitudinal magnetization component (i.e., the component along the \vec{H} direction) irrespective of the array orientation. Since it is not possible to obtain the absolute magnetization from MOKE, the reverse and forward saturation magnetizations are used in each measurement for normalization purposes. During the experiment, the angle θ_a between the array axis and the external field \vec{H} can be varied with a rotating stage as shown in the inset of Fig. 1.

III. EXPERIMENTAL RESULTS

Major hysteresis loops measured with array (i) for three different angles θ_a are presented in Fig. 2. In each measurement, the external magnetic field is increased from an initial negative saturation of -75 mT to a positive one of 75 mT, and then decreased. The MOKE signal is measured with 1 mT intervals. All curves exhibit onion-to-vortex transitions at $H \cong 0 - 8$ mT, and vortex-to-onion transitions at $H \cong 38 - 40$ mT. The transition fields, and in particular the onion-to-vortex transition field, vary with θ_a . The inset of Fig. 2 shows the onion-to-vortex transition field as a function of θ_a . This plot is obtained by averaging the transition fields

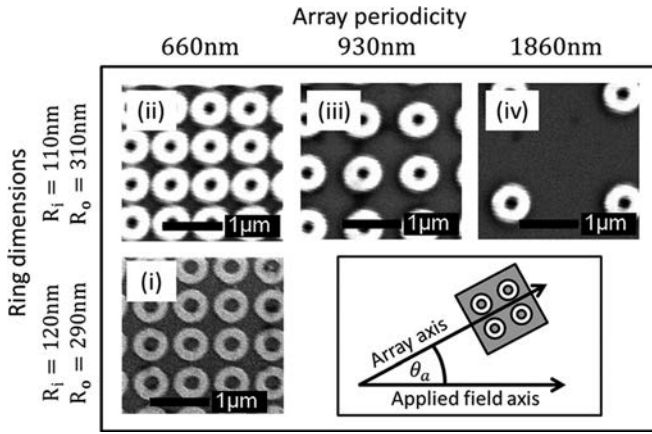


FIG. 1. Electron microscope images of the four Permalloy ring arrays used in the experiment and their respective geometries. The size of each array is $50 \mu\text{m} \times 50 \mu\text{m}$, and the total number of rings changes as a function of periodicity. The inset shows the experimental geometry: the magnetic field axis is always parallel to the measurement axis. The angle θ_a between the array axis and the field axis is variable.

at the two sides of the hysteresis loop measured from array (i) for $0^\circ < \theta_a < 65^\circ$ with $\sim 5^\circ$ steps. The onion-to-vortex transition field is defined as the field at which $M_x/M_s = 0.5$.

Hysteresis curves for $\theta_a = 0^\circ, 45^\circ$, measured with arrays (ii)-(iv), are shown in Fig. 3. Array (ii) exhibits a similar anisotropy to array (i). The effect decreases in the sparser array (iii), and vanishes completely in the sparsest one (iv). Fig. 3(d) shows a hysteresis curve obtained from a micromagnetic simulation using the NMAG software package.¹² The simulated array is a 2×2 square array with the geometric parameters of array (i) and periodic boundary conditions. The anisotropy is qualitatively reproduced by the simulation. Similar results were obtained using the OOMMF package.¹³ Both micromagnetic

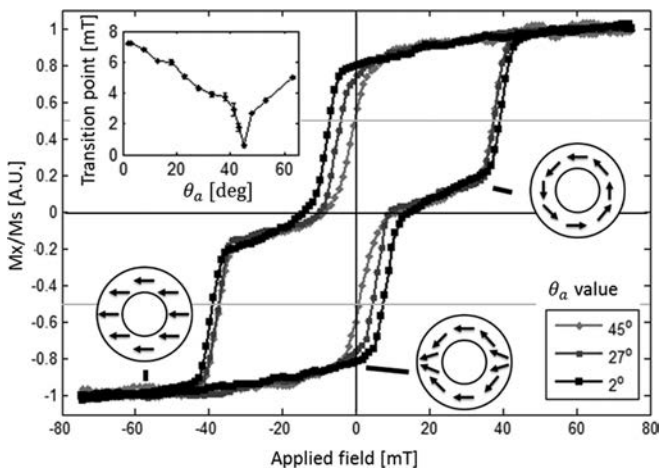


FIG. 2. MOKE hysteresis loops measured from array (i) for different θ_a values. A 45° rotation results in a ~ 8 mT decrease in the field required for the onion-to-vortex transition. The schematic diagrams show typical magnetization configurations: saturated state, onion, and vortex. In the saturated state, all magnetic moments align along the applied magnetic field direction. In the onion state, magnetic moments align parallel to the edges of the ring in the direction of the previously applied field, with two domain walls separating the domains. The vortex state is a single-domain state, where the magnetization forms a circle inside the ring. The inset at the upper left shows the dependence of the onion-to-vortex transition field on θ_a .

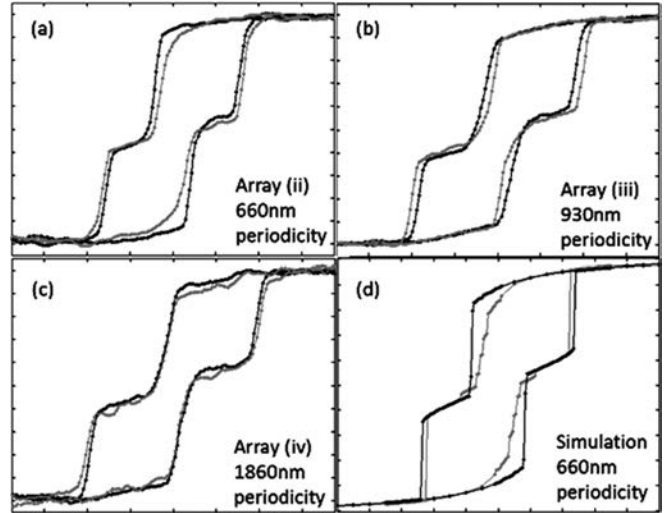


FIG. 3. (a)–(c) Hysteresis curves of arrays (ii)–(iv) for $\theta_a = 0^\circ$ (black), and $\theta_a = 45^\circ$ (gray). The data shows that the anisotropy decreases with increasing periodicity, and that the effect vanishes completely in the sparsest array. (d) Simulation results for a 2×2 rings array with the geometry of array (i) and periodic boundary conditions are also presented. The simulation qualitatively reproduces the anisotropy effect.

simulators numerically solve the dynamic Landau-Lifshitz-Gilbert (LLG) equation in order to obtain the correct micromagnetic configuration. The simulations were conducted in a manner that replicates the experiment, i.e., starting from the negative saturation field, relaxing the simulation, and raising the field in small steps until reaching the positive saturation field. In this process, the solution of each step serves as the initial condition for the following one. No specific models were built.

In addition to the major hysteresis loops described above, we also measured minor hysteresis loops. A schematic plot of a minor hysteresis loop is presented in Fig. 4(a). During the experiment, the applied field is raised from the negative saturation (A), to a certain point along the onion to vortex transition (C), and is then lowered back. The different parts of the loop correspond to different processes taking place in the sample: In sections (A and B), there is no onion to vortex switching, and the magnetization change is only due to domain wall rotation or similar reversible processes in the rings. This is validated by the fact that unless point (B) is crossed, the magnetization is single valued as a function of the applied field, without hysteresis. In sections (B and C), the rings switch from the onion to the vortex state. Sections (C and D) have an almost identical slope to (A and B), which suggests that no rings switch back and only reversible processes contribute to the magnetization change. Thus, the average height of a minor loop, normalized by the highest loop (corresponding to the entire array switching to the vortex state) is a measure of the fraction of rings that switched to the vortex state as function of the applied field. Fig. 4(b) shows the minor loops measured from array (i) for $\theta_a = 0^\circ, 45^\circ$. Note that the largest minor loop only covers the lower half of a major loop, since it is used to study the onion to vortex transition. Fig. 4(c) shows the derived number of rings in vortex state versus the applied field.

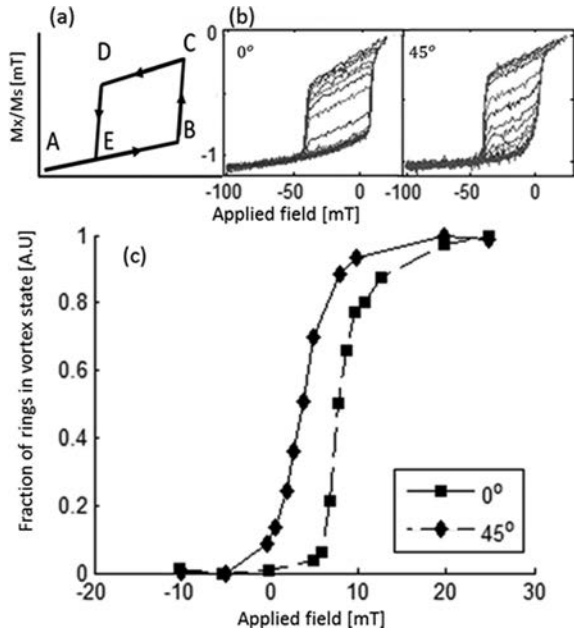


FIG. 4. (a) A schematic plot of a minor hysteresis loop. The different sections are: (A and B) magnetization changes mainly due to domain wall rotation and similar reversible processes. (B and C) magnetization changes due to onion to vortex switching. (C and D) magnetization changes again due to reversible processes. (D and E) magnetization changes due to vortex to onion switching. (b) Raw data from minor hysteresis loop measurements from which the curves are deduced. The value of n_v is derived by measuring the average height of each minor loop and normalizing it by the maximum height. This method allows the discrimination between magnetization changes due to vortex-to-onion transitions and magnetization changes due to other processes. Note that the area of the largest minor loop corresponds to the lower half of a major loop. (c) The number of rings in the vortex state, n_v , for $\theta_a = 0^\circ, 45^\circ$, as a function of the applied field.

IV. DISCUSSION

Previous studies⁴ as well as our own extensive micro-magnetic simulations show that the onion to vortex state switching in a single ring occurs by having the two domain walls move towards each other and annihilate. Snapshots of the simulation of this process are depicted in Fig. 5(a). We attribute the angular anisotropy of the switching to the dipolar interactions between domain walls of nearest-neighbor rings. We propose that when $\theta_a \rightarrow 0^\circ$ the domain walls in adjacent rings stabilize each other through the dipolar interaction and thereby hinder the annihilation process, while at $\theta_a \rightarrow 45^\circ$ the interaction induces a domain wall rotation process that results in annihilation and switching. An illustration of this process is shown in the simulation snapshots presented in Figs. 5(b) and 5(c). Both snapshots are taken close to remanence, just before the first ring switches to the vortex state. Note that in Fig. 5(b), where $\theta_a = 0^\circ$, the domain walls are still aligned along the applied field direction, due to the dipolar interaction. On the other hand, in Fig. 5(c), at $\theta_a = 45^\circ$, some of the domain walls are rotated to align with their neighbors and away from the applied field axis, thus assisting the transition to the vortex state.

This mechanism is consistent with all of the experimental data presented so far. The measurements on arrays (ii)-(iv), presented in Fig. 3, show that the anisotropy decreases and eventually vanishes as the distance between rings increases.

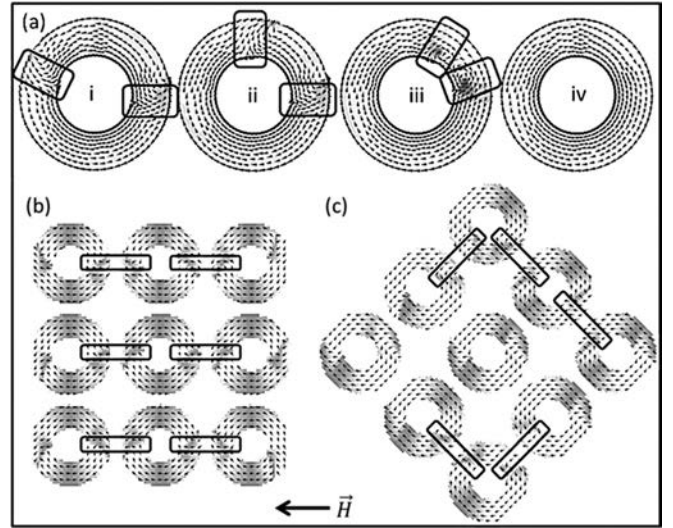


FIG. 5. (a) Snapshots from a simulation of the onion-to-vortex transition process for a single ring showing the following stages: (i) The domain walls are aligned with the applied field direction; (ii) one of the walls moves toward the other; (iii) the domain walls annihilate each other; (iv) a vortex state forms. (b) A snapshot from a simulation of an array with $\theta_a = 0^\circ$, just before the first ring switches. The domain walls align with each other along the axis of the applied field, and thus hinder the onion-to-vortex transition. (c) A snapshot from a simulation of an array with $\theta_a = 45^\circ$, just before the first ring switches. In this case, the domain walls are rotated away from the axis of the applied field, to align with their near neighbors.

This serves to establish the dipolar origin of the anisotropy. Alternative causes for the anisotropy, such as crystalline anisotropy or mechanical stress, can be ruled out since they would not exhibit such a dependence on the periodicity. In addition, this mechanism is consistent with the sharp notch around $\theta_a = 45^\circ$ in the angular dependence of the onion-to-vortex transition presented in the inset of Fig. 2. At this angle, there is a high probability that the two domain walls will align along orthogonal array axes prior to switching, as in the case of the bottom ring of Fig. 5(c). Such an alignment assists the switching process by significantly decreasing the separation between domain walls.

Further support of the hypothesis that the switching process is affected by the dipolar interactions is obtained from a detailed analysis of the minor and major hysteresis loops. Our analysis allows separation of the onion-to-vortex transition from other processes that contribute to the total magnetization change. The observed magnetization change can be described as follows:

$$\Delta M_x(H, \theta_a) = n_o \times f_o(H, \theta_a) + n_v \times f_v(H, \theta_a). \quad (1)$$

Here, ΔM_x denotes the total change of the magnetization, as measured in a major loop experiment, $n_{o(v)}$ denotes the fraction of rings in the onion (vortex) state, as derived from the minor loops experiment, and $f_{o(v)}$ is the response function of a single onion (vortex) ring to the magnetic field. Since the onion-to-vortex transition occurs in a narrow field range in the vicinity of $H = 0$, a linear behavior of $f_{o(v)}$ is assumed

$$f(H, \theta_a) \cong a(\theta_a)H + b(\theta_a). \quad (2)$$

When Eq. (2) is substituted into Eq. (1) the equation becomes

TABLE I. Fitting results.

	a_o	a_v	b_o	b_v
45°	0.015 ± 0.002	0.0047 ± 0.0003	-0.74 ± 0.02	-0.12 ± 0.01
0°	0.0048 ± 0.00	0.0052 ± 0.0005	-0.85 ± 0.01	-0.12 ± 0.02

$$\Delta M_x(H) = n_o(a_o H + b_o) + n_v(a_v H + b_v), \quad (3)$$

where all the parameters depend on the alignment angle of the array, θ_a . This simplification allows us to fit the right hand side of Eq. (3) to ΔM_x and obtain the values of a_o, b_o, a_v, b_v as fitting parameters. The results are presented in Table I.

The results show a significant difference between the behavior of a single ring in the aligned and rotated arrays below the onion-to-vortex transition. First and foremost, the ratio of magnetization slopes between the rotated 45° and aligned 0° states is very different between the onion and vortex states $a_o(45^\circ)/a_o(0^\circ) = 3.125$. This is shown in Fig. 3(a) where the rotated array has an early but slow increase in magnetization as the domains walls move inside the ring and approach the vortex state. The behavior is contrasted with the unrotated array, where there is practically no magnetization change due to the dipolar pinning until the transition point is reached. At that point, there is a very sharp change in the magnetization as the onion changes to the vortex state. The attribution of this effect to the domain wall movement and not to some other magnetic reconfiguration is further supported by the fact that $a_v(45^\circ) = a_v(0^\circ)$ (within experimental error) which shows the absence of an effect on the vortex-state rings where there are no domain walls.

The $b_{o/v}$ fitting coefficients give information about the remanent configurations of the rings. Rings in the vortex state have perfect polar symmetry, and when the anisotropic effect of the external field is removed, there should be no difference whatsoever between the vortex configurations in aligned and rotated arrays. Indeed in the vortex state $b_v(45^\circ) = b_v(0^\circ)$. This proves that the angular anisotropy is introduced either by the external field or by the array, through the domain wall coupling. When both mechanisms are removed complete angular isotropy is restored.

If the domain walls in the onion state were perfect dipoles, all aligned along the array axes at remanence, one would expect the ratio $b_o(45^\circ)/b_o(0^\circ)$ to be $\sin(45^\circ) = 1/\sqrt{2}$. The actual measured ratio is $b_o(45^\circ)/b_o(0^\circ) = 0.87$, which indicates an effective rotation of $\sim 30^\circ$. The slightly smaller than expected effective rotation can be attributed to partial rotation

of the onion state in some of the rings, or of the individual domain walls as in Fig. 5 (a-iii). The $\sin(45^\circ)$ ratio is probably the theoretical upper limit.

V. SUMMARY

In summary, we found an angular anisotropy in the onion-to-vortex transition in dense ferromagnetic ring arrays with up to 8 mT changes in the switching field as a function of array orientation. The data imply that this anisotropy arises from dipolar interactions between domain walls of adjacent rings in the onion state. We show that in arrays aligned with the external field, the interaction stabilizes the walls and thus sharpens the switching process. On the other hand, in rotated arrays the nearest neighbor domain walls assist domain wall rotation thereby also assisting the switching process ultimately making the transition wider. The phenomenon is also qualitatively reproduced in numerical micromagnetic simulations. This effect should be a significant consideration in the design of any application that requires dense ferromagnetic ring arrays.

ACKNOWLEDGMENTS

We would like to thank Siming Wang for useful discussions. This work was supported by the US AFOSR under Grant No. FA9550-10-1-0409.

- ¹M. Kläui, C. Vaz, L. Lopez-Diaz, and J. Bland, *J. Phys.: Condens. Matter* **15**, R985 (2003).
- ²P. Landeros, J. Escrig, D. Altbir, M. Bahiana, and J. d'Albuquerque e Castro, *J. Appl. Phys.* **100**, 044311 (2006).
- ³M. Beleggia, J. Lau, M. Schofield, Y. Zhu, S. Tandon, and M. Degraef, *J. Magn. Magn. Mater.* **301**, 131 (2006).
- ⁴W. Zhang and S. Haas, *Phys. Rev. B* **81**, 064433 (2010).
- ⁵M. Kläui, C. Vaz, L. Heyderman, U. Rudiger, and J. Bland, *J. Magn. Magn. Mater.* **290**, 61 (2005).
- ⁶M. Kläui, C. Vaz, J. Bland, L. J. Heyderman, F. Nolting, A. Pavlovskaya, E. Bauer, S. Cherifi, S. Heun, and A. Locatelli, *Appl. Phys. Lett.* **85**, 5637 (2004).
- ⁷M. Kläui, C. Vaz, J. Bland, and L. J. Heyderman, *Appl. Phys. Lett.* **86**, 032504 (2005).
- ⁸T. Miyawaki, K. Toyoda, M. Kohda, A. Fujita, and J. Nitta, *Appl. Phys. Lett.* **89**, 122508 (2006).
- ⁹M. Kohda, K. Toyoda, T. Miyawaki, A. Fujita, and J. Nitta, *J. Appl. Phys.* **103**, 07A714 (2008).
- ¹⁰N. Qureshi, S. Wang, M. A. Lowther, A. R. Hawkins, S. Kwon, A. Liddle, J. Bokor, and H. Schmidt, *Nano Lett.* **5**, 1413 (2005).
- ¹¹M. Natali, A. Lebib, Y. Chen, I. L. Prejbeanu, and K. Ounadjela, *J. Appl. Phys.* **91**, 7041 (2002).
- ¹²H. Fangohr, G. Bordignon, M. Franchin, A. Knittel, P. A. J. de Groot, and T. Fischbacher, *J. Appl. Phys.* **105**, 07D529 (2009).
- ¹³M. J. Donahue and D. G. Porter, "OOMMF User's Guide," Version 1 Intergracy Report No. NISTIR 6376 Nist, Gaithersburg, MD, 1999.